JOURNAL OF MEDICAL MICROBIOLOGY

SHORT COMMUNICATION

Larcombe *et al.*, *Journal of Medical Microbiology* 2020;69:290–297

DOI 10.1099/jmm.0.001163

MICROBIOLOGY SOCIETY

OPEN MICROBIOLOGY

A mouse model of *Staphylococcus aureus* small intestinal infection

Sarah Larcombe[1], Jhih-Hang Jiang[1], Melanie L. Hutton[1], Helen E. Abud[2], Anton Y. Peleg[1,3] and Dena Lyras[1,*]

Abstract

Introduction. *Staphylococcus aureus* is a recognised cause of foodborne intoxication and antibiotic-associated diarrhoea (AAD), which are both mediated by staphylococcal enterotoxins. However, unlike foodborne intoxication, AAD appears to require infection of the host. While *S. aureus* intoxication is widely studied, little is known about *S. aureus* pathogenesis in the context of gastrointestinal infection.

Aim. To develop a mouse model of *S. aureus* gastrointestinal infection.

Methodology. An established AAD mouse model was adapted for *S. aureus* infection, and damage observed via histopathological analysis and immunostaining of intestinal tissues.

Results. Various strains colonised the mouse model, and analysis showed that although clinical signs of disease were not seen, *S. aureus* infection induced damage in the small intestine, disrupting host structures essential for epithelial integrity. Studies using a staphylococcal enterotoxin B mutant showed that this toxin may contribute to damage during gastrointestinal infection.

Conclusion. This work presents a new mouse model of *S. aureus* gastrointestinal infection, while also providing insight into the pathogenesis of *S. aureus* in the gut.

INTRODUCTION

Staphylococcus aureus is a known cause of food poisoning, which is the result of intoxication following the ingestion of food containing pre-formed staphylococcal enterotoxins (SEs) [1]. *S. aureus* is also a lesser known cause of antibiotic-associated diarrhoea (AAD), which often presents as enterocolitis with large volumes of watery diarrhoea [2–7]. Unlike food poisoning, *S. aureus* AAD is a gastrointestinal infection that often occurs following antibiotic-induced dysbiosis of the intestinal microbiota [8]. However, due to the focus on *Clostridioides difficile* as the major cause of AAD there is consequently a lack of screening for other aetiologies. Because of this, the burden of *S. aureus* in AAD is relatively unknown, and little is known about the pathogenesis of *S. aureus* during gut infection.

Most *S. aureus* strains isolated in AAD cases are methicillin resistant, and produce more than one SE [6, 9], which are pyrogenic exotoxins with superantigenic activity [1]. Mice have a reduced sensitivity to SEs compared to humans due to differences in their MHC class II receptor molecules [10, 11], and require a higher dose to see a comparative effect. For this reason, SEs are commonly assessed using murine intoxication models using purified toxin [12, 13]. Mouse models are also used to assess *S. aureus* gastrointestinal colonisation, commonly involving pre-treatment of mice with antibiotics to reduce endogenous gut microbiota and induce susceptibility to *S. aureus* colonisation [14–16], followed by oral inoculation with *S. aureus* [14, 17, 18], however gastrointestinal disease is rarely considered in these studies.

To address the lack of available animal models for the study of *S. aureus* gastrointestinal disease, we hypothesised that a well-established *C. difficile* mouse model of infection [19]

Received 04 June 2019; Accepted 16 January 2020; Published 31 January 2020

Author affiliations: [1]Infection and Immunity Program, Monash Biomedicine Discovery Institute and Department of Microbiology, Monash University, Clayton, Victoria, Australia; [2]Cancer Program, Monash Biomedicine Discovery Institute and Department of Anatomy and Developmental Biology, Monash University, Clayton, Victoria, Australia; [3]Department of Infectious Diseases, The Alfred Hospital and Central Clinical School, Monash University, Melbourne, Victoria, Australia.

***Correspondence:** Dena Lyras, dena.lyras@monash.edu

Keywords: *Staphylococcus aureus*; antibiotic-associated diarrhoea; infection model; mouse model; gastrointestinal infection; bacterial pathogenesis.

Abbreviations: AAD, Antibiotic-associated diarrhoea; SE, Staphylococcal enterotoxin; SEB, Staphylococcal enterotoxin B.

S. aureus RN8098 genome sequence: NCBI BioProject no. PRJNA430465.

One supplementary table and two supplementary figures are available with the online version of this article.

001163 © 2020 Not applicable

that has previously been adapted for the study of non-*C. difficile* AAD [20] could be adapted for the study of *S. aureus* gastrointestinal infection in the context of the dysbiotic gut. Thus in this study, we aimed to establish this model and use it to explore the pathogenesis of *S. aureus* in the gut and the role of specific virulence factors. *S. aureus* colonisation in this model was confirmed using several strains. Further analysis was performed using the *S. aureus* strain RN8098 [21], which produces staphylococcal enterotoxin B (SEB), a SE that is known to induce intestinal permeability, tissue damage, and inflammation in the gut following intraperitoneal injection of purified toxin [13, 22]. This work showed that *S. aureus* RN8098-mediated gut damage could be observed in the proximal and mid-small intestine, and provided insight into the pathways of damage caused by *S. aureus* during gastrointestinal infection using immunostaining for specific markers.

METHODS

Bacterial culture conditions

S. aureus was cultured aerobically in heart infusion (HI) broth (Oxoid) with agitation, or HI agar at 37 °C. To prepare the inoculum for mouse infection, 20 ml HI broth was inoculated with an overnight broth culture to a starting OD_{600} of 0.3, and grown to an OD_{600} of 1.0. Cells were harvested by centrifugation at 10000 ***g*** for 3 min, washed once with PBS, and then resuspended in PBS to a final concentration of 10^8 c.f.u. ml^{-1}.

Complementation of the *S. aureus* RN8098 *seb* mutant

The *seb* gene with 500 bp of upstream sequence was cloned from *S. aureus* RN8098 genomic DNA into the plasmid pALC2073 [23] using forward primer 5′ GCAAGGTACCAA CCTAGTGATCGTTTAAAAGC 3′ and reverse primer 5′ GCAAGAATTCTCACTTTTTCTTTGTCGTAAGAT 3′. The plasmid pALC2073-*seb* was propagated in *S. aureus* RN4220 [24], re-isolated using QIAprep Spin Miniprep Kit (QIAGEN; as per manufacturer's instructions), and then electroporated into the *S. aureus* RN8098 *seb* mutant, as described previously [25]. Complementation was confirmed by PCR using forward primer 5′ GGGGATGTGCTGCAAGGCGAT 3′ and reverse primer 5′ TGGATCCCCTCGAGTTCATGAAAAAC 3′, which flank the insertion region of pALC2073, followed by nucleotide sequencing of the PCR product.

SDS-PAGE and Western blot

Culture supernatants from all *S. aureus* RN8098 derivative strains were separated by 12% sodium dodecyl sulfate-polyacrylamide gel electrophoresis (SDS-PAGE) and transferred onto a nitrocellulose membrane. SEB was detected using anti-SEB rabbit polyclonal antibody (Abcam) at a concentration of 1 μg ml^{-1}, followed by a goat anti-rabbit IgG-HRP conjugate (Millipore; 1:10000 dilution). Antibody binding was detected using Western Lightning Chemiluminescence reagent kit (Perkin-Elmer) as per manufacturer's instructions, and imaged using a Biorad Chemidoc system.

Murine model of non-*C. difficile* AAD

Animal experimentation was performed in accordance with Victorian State Government regulations and approved by the Monash University Animal Ethics Committee (AEC no. MARP/2014/145). Male 6–7 week old C57BL/6J mice (Walter and Eliza Hall Institute of Medical Research) were pre-treated with an antibiotic cocktail in the drinking water consisting of kanamycin (0.6 mg ml^{-1}), gentamicin (0.0525 mg ml^{-1}), colistin (1275 U ml^{-1}), metronidazole (0.3225 mg ml^{-1}), vancomycin (0.0675 mg ml^{-1}) and cefaclor (0.45 mg ml^{-1}) for 7 days, ceasing three days prior to inoculation to ensure that no residual antibiotic was present in the mice that may affect *S. aureus* colonisation. Each mouse was inoculated with approximately 10^7 c.f.u. by oral gavage, with one antibiotic pre-treated group left uninfected per experiment (referred to throughout as 'uninfected'). Prior to inoculation, faecal pellets from each group were screened to confirm the absence of *S. aureus* and *C. difficile* by plating on Mannitol Salt Agar (MSA; Merck) and CHROMID *C. difficile* agar (bioMérieux), followed by incubation at 37 °C for 48 h, under aerobic and anaerobic conditions, respectively. Throughout the course of infection, mice were monitored for weight loss, faecal consistency, and behavioural changes including alertness, movement and activity level. To enumerate bacterial shedding, faeces was collected at 24 h intervals, followed by resuspension in PBS at 100 mg ml^{-1}. Serial dilutions were plated on MSA and incubated at 37 °C for 48 h. *In vivo* retention of the *seb* complementation vector in mice infected with the *seb* complement strain was confirmed by patching 100 colonies per time point onto HI agar supplemented with 10 μg ml^{-1} chloramphenicol. Animals were humanely euthanised by CO_2 asphyxiation at defined endpoints. For time course analysis, one group of five mice was humanely euthanised at each time point up to 96 h post-inoculation. For all other infection trials, mice were humanely euthanised at 48 h post-inoculation. Following euthanasia, faecal pellets from each group of mice were again screened for *C. difficile*, and all uninfected mice were also screened for *S. aureus*, as described previously. Intestinal tissues were collected from each mouse and Swiss-rolled [26] prior to fixation in 10% neutral-buffered formalin, and then processed, paraffin-embedded, and sectioned at 4 μm.

Histological staining and scoring

Intestinal sections were stained with haematoxylin and eosin (H&E) using standard techniques. Imaging was performed using the Aperio Scanscope AT Turbo slide scanner and Aperio ImageScope version 12 software. Histological damage scoring was performed blinded as described previously [20], where the length of each tissue section was measured, followed by length measurements of areas showing histological damage, which included structural damage to the mucosa/sub-mucosa, alterations to villus and crypt architecture, inflammation, and oedema. Histological damage scores are presented as a percentage of total tissue damaged.

Immunostaining

Immunostaining and imaging of E-cadherin, β-catenin, ezrin and proliferating cell nuclear antigen (PCNA) was performed as described previously [20]. Analysis of cellular proliferation and intestinal crypt density performed on PCNA-stained sections was also performed as described previously [20], except that at least 100 fields of view were counted per group.

Isolation of genomic DNA and sequencing

S. aureus RN8098 wild-type strain genomic DNA was isolated using the QIAGEN DNeasy Blood and Tissue kit, as per manufacturer's instructions. Sequencing libraries were prepared with Nugen, Ovation Ultraflow System V2 (1–96) using protocol M01380v1, 2015. Sequencing was performed using Illumina MiSeq v2 to achieve paired end 150 bp reads. *De novo* genome assemblies were prepared using SPAdes and annotated using Prokka. The identities of proteins of interest were confirmed using NCBI BLASTp. Multi-locus sequence typing (MLST) was performed using Centre for Genomic Epidemiology (CGE) MLST 1.8 [27], and *spa* typing was performed using CGE spaTyper 1.0 [28]. The *S. aureus* RN8098 genome sequence can be accessed under BioProject no. PRJNA430465.

Statistical analysis

Statistical significance of data was determined by the Kruskal-Wallis test with Dunn's multiple comparisons test or Mann Whitney *U* test, performed using GraphPad Prism 7.

RESULTS AND DISCUSSION

Intestinal colonisation can be achieved by diverse *S. aureus* strains in a mouse infection model

Despite the clinical importance of *S. aureus*, little is known about its pathogenesis in the context of gastrointestinal infection, which may be attributed to a lack of suitable animal models. Therefore, the widely-used infection model for *C. difficile* AAD [19, 29–31] was adapted for use in this study, with preliminary experiments utilising the commonly studied *S. aureus* strains SF8300 [32] and JH1 [33], as well as the SEB-producing strain RN8098 [21].

Results showed that colonisation could be achieved after inoculation of antibiotic pre-treated mice with 10^7 c.f.u. of any strain, with faecal shedding detected at each 24 h interval tested post-inoculation (Fig. 1a). Colonisation levels were highest at 24 h post-inoculation, and dropped significantly

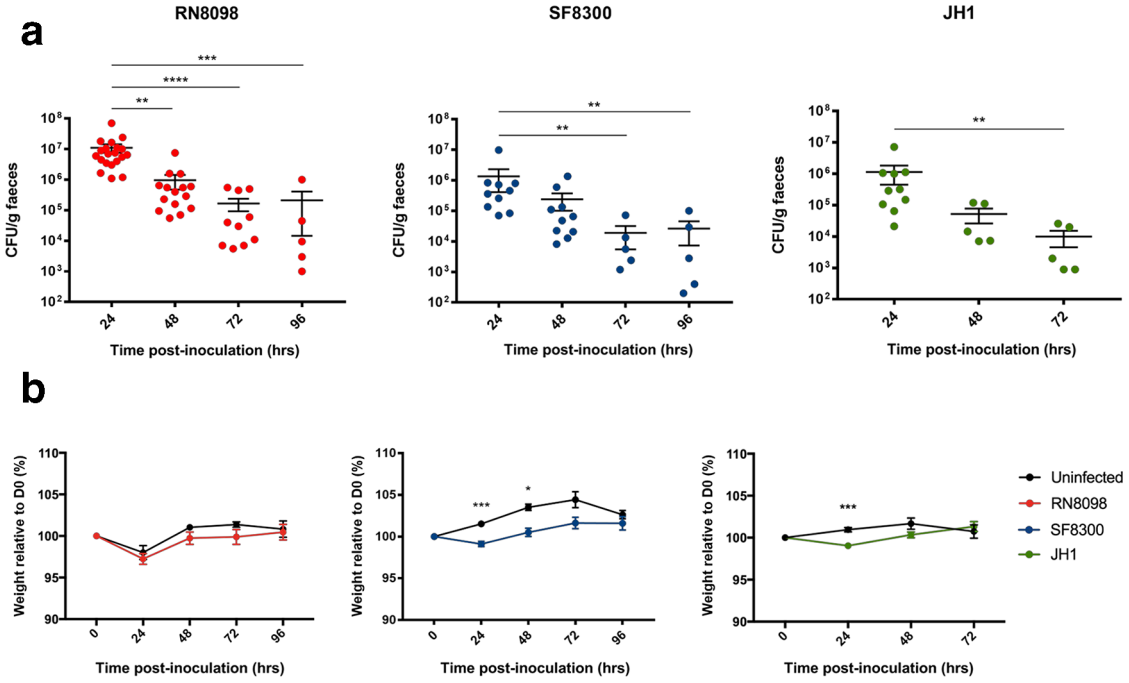

Fig. 1. Time course analysis of faecal shedding (a) and weight loss (b) of mice infected with *S. aureus* strains RN8098, SF8300, or JH1. (a). Faecal samples were collected at 24 h intervals from mice inoculated with each strain. Faecal shedding is presented as c.f.u./g of faeces, with each data point representing an individual mouse. Error bars=Mean± SEM; *n*=5–20 mice (RN8098=20, with 5 humanely euthanised per time point; SF8300=10, with 5 humanely euthanised at 48 h post-inoculation; JH1=10, with 5 humanely euthanised at 24 h post-inoculation). Statistical significance was determined using the Kruskal-Wallis test with Dunn's multiple comparisons test (***P*≤0.01, ****P*≤0.001, *****P*≤0.0001). (b). Uninfected and infected mice were weighed prior to inoculation and at 24 h intervals post-inoculation. Weight loss is presented as a percentage loss relative to weight on the day of inoculation (day 0, D0). Error bars=Mean± SEM; *n*=4–20 mice per group (infected mice numbers as above; RN8098 uninfected control=4; SF8300 uninfected control=5; JH1 uninfected control=10). Significant difference from uninfected was determined using the Mann Whitney *U* test (**P*≤0.05, ****P*≤0.001).

over time for all strains (Fig. 1a), which is expected as the normal gut microbiota recovers in the absence of antibiotic treatment [34, 35]. Of note, when colonisation of inoculated bacteria is not achieved, they are cleared from the gut within 24 h, and cannot be detected in the faeces (unpublished data). However, *S. aureus* infection did not appear to induce severe clinical signs of disease, with all infected mice increasing in weight over the course of infection following an initial weight loss at 24 h post-inoculation (Fig. 1b). No change in behaviour was observed in mice infected with any strain, and mice did not develop fulminant diarrhoea, however soft, unformed faeces were observed in infected mice only. The subtlety of these clinical symptoms is in line with the previous adaptation of this model for non-*C. difficile* AAD pathogens [20], and therefore further analysis is likely required for the delineation of disease outcomes in this model.

S. aureus causes gastrointestinal damage in a mouse infection model

To observe and define the damage caused by *S. aureus* in this model, and to explore the contribution of SEB to this damage, further experiments were performed using *S. aureus* RN8098 in comparison to an isogenic *seb* mutant [21] and complemented mutant (this study). Prior to mouse infection trials, complementation of the *seb* mutant was confirmed *via* PCR (Fig. S1, available in the online version of this article), with the *seb* complement showing the expected band size of approximately 1.5 kb, and sequencing confirming the correct nucleotide sequence (not shown), confirming the carriage of pALC2073 with the *seb* gene insertion. SEB production by the complemented *seb* mutant was then confirmed in comparison to the wild-type and *seb* mutant strains by Western blot (Fig. S2). Despite the lack of obvious clinical signs of disease seen in this model previously, histological analysis of intestinal tissues from infected mice revealed that *S. aureus* RN8098 wild-type infection resulted in damage in the proximal small intestine. This damage presented as disruption to intestinal epithelial cells with sporadic loss of nuclei staining, development of a subepithelial gap in the villi, villus blunting, and destruction of crypts and overall tissue architecture in sections (Fig. 2b). Damage in the mid-small intestine was less prevalent and less severe, presenting primarily as surface epithelial damage and villus blunting (Fig. 2b). Damage was most severe at 48 h post-inoculation, and did not appear to obviously affect the distal small intestine, caecum, or colon (data not shown). This result supports a previous observation that *S. aureus* does not induce damage to the ileum or colon of mice following intravenous inoculation and dissemination to the gut, however proximal and mid-small intestinal tissues were not analysed [36]. Of note, increasing the inoculum of *S. aureus* RN8098 from 10^7 c.f.u to 10^9 c.f.u failed to obviously increase clinical signs of disease, or the level of histological damage observed (data not shown). Therefore, it is apparent that *S. aureus* gastrointestinal infection in this model presents as a subclinical disease, with infection-mediated damage evident via histological analysis of small intestinal tissues from infected mice in comparison to antibiotic pre-treated, uninfected mice.

Consistent with previous results for the wild-type strain, colonisation was achieved in mice infected with the RN8098 *seb* mutant and complemented strains, with a significant difference in colonisation levels at 24 vs. 48 h ($P \leq 0.01$), and no reduction in weight when compared to uninfected mice (Fig. 2a). Infection by the *seb* mutant and *seb* complement strains induced similar histopathological signs in the proximal and mid-small intestine to the wild-type infection, such as damage to the epithelial surface and loss of nuclei staining (Fig. 2b). Scoring the level of histological damage caused by all RN8098-derivative strains revealed that SEB-mediated damage during infection with *S. aureus* RN8098 could be detected in the proximal small intestine, with results showing that the *seb* mutant induced significantly less damage in comparison to the wild-type ($P \leq 0.05$) and *seb* complement ($P \leq 0.01$) strains (Fig. 2c), however damage in the mid-small intestine was induced to a similar level by all infecting strains (Fig. 2c).

These results suggest that SEB contributes to gastrointestinal damage during infection by *S. aureus* RN8098 in this model, providing evidence for the first time of the involvement of SEB during gastrointestinal infection rather than intoxication. However, the damage induced by the *seb* mutant implicates the involvement of virulence factors other than SEB in the gastrointestinal damage caused by *S. aureus* RN8098 infection, highlighting the difficulty of defining the contribution of specific *S. aureus* virulence factors in an infection model.

S. aureus disrupts markers of gastrointestinal epithelial integrity in a mouse infection model

To determine whether the *S. aureus*-mediated damage observed in this model affected the integrity of the gastrointestinal epithelium, immunostaining was performed for specific markers, including the adherens junction proteins E-cadherin and β-catenin. These proteins are essential for the maintenance of structural integrity of the gut epithelium, providing a physical barrier between the lumen of the gut and the basolateral membrane [37]. This analysis revealed disruption to E-cadherin and β-catenin along the length of the villi in the proximal and mid-small intestine of mice infected by all RN8098 derivative strains including the *seb* mutant (Fig. 3a), despite the known ability of SEs to reduce the expression of adherens junction proteins [13, 38, 39]. For all strains, this damage was more prevalent in the proximal small intestine, affecting both E-cadherin and β-catenin or β-catenin alone in some areas (Fig. 3a). In the mid-small intestine, adherens junctions were intact in the majority of the tissue analysed, however damage appeared in small patches, often only affecting β-catenin (Fig. 3a).

The integrity of adherens junctions is also tightly linked with the maintenance of apical integrity due to associations between the cellular polarity protein ezrin and the actin cytoskeleton [40]. It is therefore unsurprising that the damage to ezrin was also induced by all infecting strains in the proximal and mid-small intestine (Fig. 3b). This damage was also more prevalent in the proximal small intestine, with

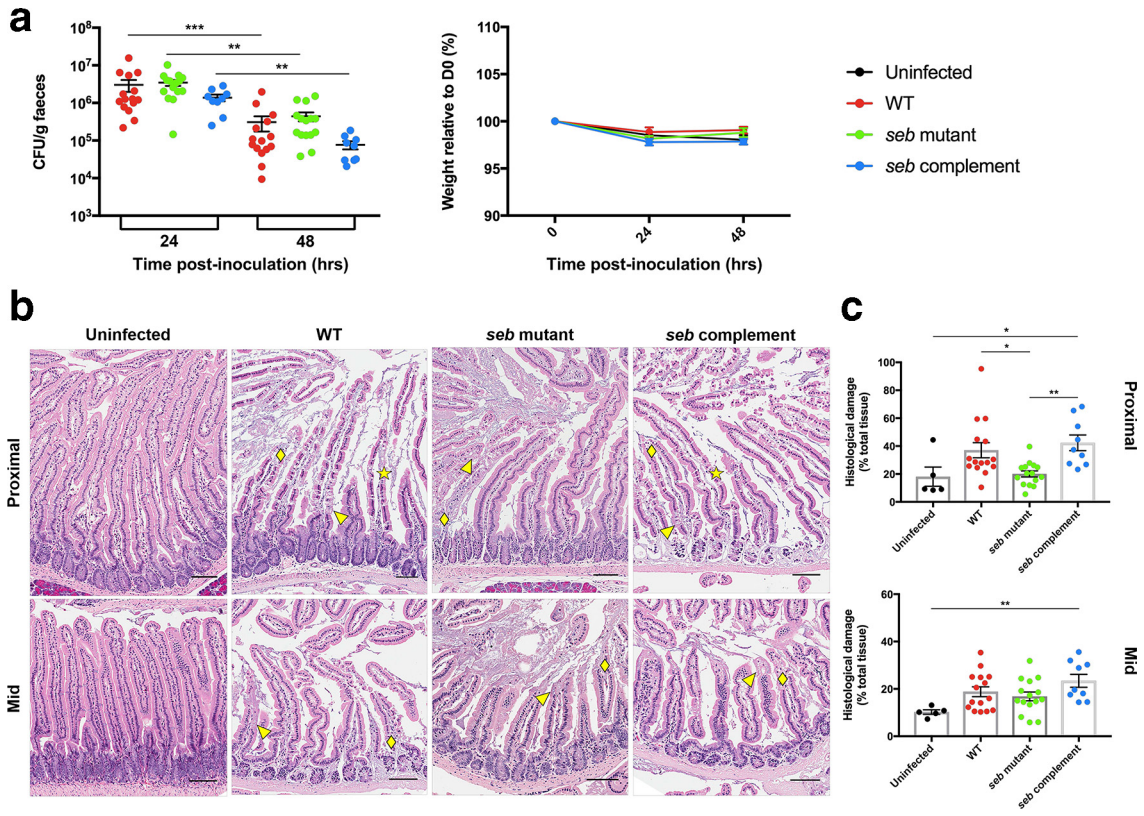

Fig. 2. Comparative analysis of *S. aureus* RN8098 WT, *seb* mutant and *seb* complemented strains in the mouse model of *S. aureus* gastrointestinal infection. (a). Faecal shedding and weight loss of mice infected with *S. aureus* RN8098 WT, *seb* mutant or *seb* complement. Faecal samples were collected at 24 h intervals from mice inoculated with each strain. Faecal shedding is presented as c.f.u./g of faeces, with each data point representing an individual mouse. For weight loss analysis, uninfected and infected mice were weighed prior to inoculation and at 24 h intervals post-inoculation. Weight loss is presented as a percentage relative to weight on the day of infection (day 0, D0). Error bars=Mean± SEM; *n*=5–15 mice per group (WT=15; *seb* mutant=15; *seb* complement=9; uninfected=5). Statistical significance was determined between different groups at the same time point, and between the same group at different time points using the Kruskal-Wallis test with Dunn's multiple comparisons test (**$P \leq 0.01$, ***$P \leq 0.001$). (b). Histological damage of small intestinal tissue following 48 h of infection with either *S. aureus* RN8098 WT, *seb* mutant, or *seb* complement. Proximal and mid-small intestine was collected from uninfected mice, and mice inoculated with either strain and stained with H&E. Triangles=loss of nuclei staining; stars=development of a subepithelial gap; diamonds=epithelial damage. Scale bar=100 µm. (c). Histological damage was scored blinded by measuring the length of each tissue, followed by measurements of areas showing histological damage, presented as a percentage of total tissue damaged. Error bars=Mean± SEM; *n*=5–15 mice per group (WT=15; *seb* mutant=15; *seb* complement=9; uninfected=5). Statistical significance was determined using the Kruskal-Wallis test with Dunn's multiple comparisons test (*$P \leq 0.05$, **$P \leq 0.01$).

much of the mid-small intestine appearing healthy with small patches of damage detected (Fig. 3b). Together, these results provide insight into the damage pathways of *S. aureus* RN8098 gastrointestinal infection, and further highlight the likely involvement of virulence factors other than SEB in the damage observed.

S. aureus alters gastrointestinal crypts in a mouse infection model

Due to the damage observed in the proximal small intestine of mice infected with *S. aureus* RN8098, we explored whether this had an effect on cellular proliferation within the stem cell niche by staining for the presence of the cellular proliferation marker PCNA (proliferating cell nuclear antigen) (Fig. 3c). This analysis revealed that infection with *S. aureus* RN8098 does not appear to affect the rate of cellular proliferation in this model, with no difference in the mean number of PCNA-positive cells per crypt detected between uninfected mice and mice infected with any strain (Fig. 3d). This analysis did reveal, however, that the density of crypts within the mucosa of damaged areas of tissue was significantly lower in mice infected with the wild-type and *seb* complement strains when compared to healthy tissue from uninfected mice ($P \leq 0.01$ and $P \leq 0.001$, respectively) (Fig. 3d). While not statistically significant, crypt density was similarly low for mice infected with the *seb* mutant in comparison to uninfected mice (Fig. 3d). This may suggest that although *S. aureus* RN8098 infection reduces crypt density, the remaining crypts appear to be healthy, providing further insight into the pathways of *S. aureus* gastrointestinal pathogenesis.

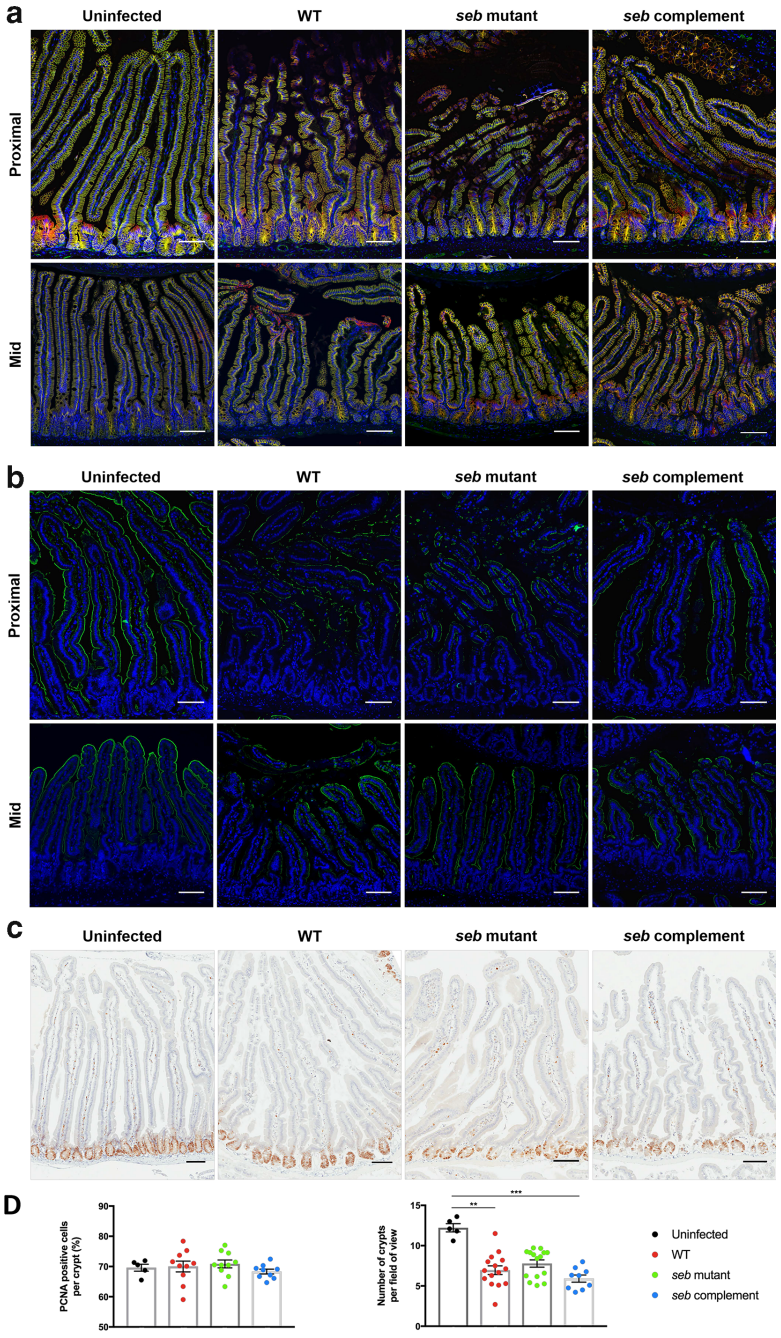

Fig. 3. Immunostaining for specific markers in the gastrointestinal mucosa for the analysis of intestinal damage. Detection of (a). adherens junction proteins E-cadherin and β-catenin and (b). cellular polarity marker ezrin in the proximal and mid-small intestine following 48 h of infection with either *S. aureus* RN8098 WT, *seb* mutant, or *seb* complement. Tissues were collected from uninfected and infected mice and immunostained with E-cadherin (red) and β-catenin (green), or ezrin (green) and counterstained with DAPI (blue). Co-localisation of E-cadherin and β-catenin shows as yellow. Scale bar=100 µm. Detection of (c). cellular proliferation marker PCNA in the proximal small intestine following 48 h of infection with either *S. aureus* RN8098 WT, *seb* mutant, or *seb* complement. Proximal small intestine was collected from uninfected and infected mice and immunostained with PCNA (brown) and counterstained with haematoxylin (blue). Scale bar=100 µm. (d). Cellular proliferation was quantified by counting the number of PCNA positive and negative cells per crypt for 30 crypts per mouse, and is presented as the percentage of PCNA positive cells per crypt. Error bars=Mean± SEM; n=5–10 mice per group (WT=10; *seb* mutant=10; *seb* complement=9; uninfected=5). Crypt density was quantified by counting the number of crypts in a defined field of view for uninfected mice in comparison with fields of view from infected mice where histological damage was observed. At least 100 fields of view were counted per group (WT=146; *seb* mutant=126; *seb* complement=102; uninfected=100), and results are presented as the average number of crypts per field of view. Error bars=Mean± SEM; n=5–15 mice per group (WT=15; *seb* mutant=15; *seb* complement=9; uninfected=5). Statistical significance was determined using the Kruskal-Wallis test with Dunn's multiple comparisons test (**P≤0.01, ***P≤0.001).

S. aureus RN8098 encodes numerous virulence factors

Given that *S. aureus* RN8098 caused damage in the small intestine of infected mice independent of SEB, we were interested in identifying what other virulence factors were encoded by this strain. Whole genome sequencing and bioinformatic analysis of *S. aureus* RN8098 (ST250, *spa* type t008) revealed the presence of numerous genes encoding putative virulence factors including adhesion factors, immune modulators, secretion systems, and siderophores (Table S1). The presence of the gene encoding SEB was confirmed, and importantly, genes encoding other toxins were detected, including the staphylococcal enterotoxin-like proteins SEK and SEQ, leucotoxins LukED and LukGH, as well as several other exotoxins and superantigen-like proteins. As noted previously, a redundancy in virulence factors capable of causing gastrointestinal damage may obfuscate the damage caused by a particular virulence factor, and as such, the complete delineation of damage caused specifically by SEB was not possible in this study, supporting the continued need for *in vitro* analyses and intoxication models in the characterisation of *S. aureus* infection. However, it is important to consider how these results will apply under infection conditions in the context of a complex *in vivo* environment, as addressed by the work in this study.

Taken together, the results of this study contribute to a more comprehensive understanding of *S. aureus* pathogenesis in the gastrointestinal tract, providing novel insight into the disruption of host processes and the role of specific virulence factors during *S. aureus* gastrointestinal infection. While *S. aureus* AAD in humans exhibits symptoms that were not seen in this model, such as large volume diarrhoea and macroscopic gut pathologies including pseudomembranes [8], it is reported to primarily affect the small intestine, which was reflected in the model established in this study. Further optimisation of this model may be achieved through changes to antibiotic pre-treatment or *S. aureus* strain selection, which are factors that have been explored successfully in the development of *C. difficile* animal models [41]. Therefore, despite exhibiting a milder form of disease compared to *S. aureus* AAD in humans, the development of a mouse model of *S. aureus* gastrointestinal infection, utilising a single oral inoculation of *S. aureus* following non-invasive antibiotic pre-treatment provides a novel platform for the analysis of *S. aureus* in the context of the dysbiotic gut, which may contribute to future studies of this multi-faceted pathogen.

Funding information
SL was supported by an Australian Government Research Training Program Scholarship and DL was supported by an Australian Research Council Future Fellowship [FT120100779]. All funding bodies had no role in study design, data collection and analysis, interpretation, preparation of the manuscript, or decision to publish.

Acknowledgements
The authors acknowledge the facilities, and scientific and technical assistance provided by the Monash Histology Platform, Department of Anatomy and Developmental Biology, Monash University; the Medical Genomics Facility, Hudson Institute of Medical Research; the Monash Bioinformatics Platform, Monash University. We also thank Professor Alan Lambowitz for the provision of *S. aureus* RN8098 wild-type and *seb* mutant strains.

Conflicts of interest
The authors declare that there are no conflicts of interest.

References

1. Argudín MA, Mendoza MC, Rodicio MR. Food poisoning and *Staphylococcus aureus* enterotoxins. *Toxins* 2010;2:1751–1773.
2. Lane AB, Copeland NK, Onmus-Leone F, Lawler JV. Methicillin-Resistant *Staphylococcus aureus* as a probable cause of antibiotic-associated enterocolitis. *Case Rep Infect Dis* 2018;2018:3106305–3.
3. Bergevin M, Marion A, Farber D, Golding GR, Lévesque S. Severe MRSA enterocolitis caused by a strain harboring enterotoxins D, G, and I. *Emerg Infect Dis* 2017;23:865–867.
4. Wei Y, Gong J, Zhu W, Guo D, Gu L *et al*. Fecal microbiota transplantation restores dysbiosis in patients with methicillin resistant *Staphylococcus aureus* enterocolitis. *BMC Infect Dis* 2015;15:265.
5. Avery LM, Zempel M, Weiss E. Case of antibiotic-associated diarrhea caused by *Staphylococcus aureus* enterocolitis. *Am J Health Syst Pharm* 2015;72:943–951.
6. Gravet A, Rondeau M, Harf-Monteil C, Grunenberger F, Monteil H *et al*. Predominant *Staphylococcus aureus* isolated from antibiotic-associated diarrhea is clinically relevant and produces enterotoxin A and the bicomponent toxin LukE-LukD. *J Clin Microbiol* 1999;37:4012–4019.
7. Lo TS, Borchardt SM. Antibiotic-associated diarrhea due to methicillin-resistant *Staphylococcus aureus*. *Diagn Microbiol Infect Dis* 2009;63:388–389.
8. Larcombe S, Hutton ML, Lyras D. Involvement of bacteria other than *Clostridium difficile* in antibiotic-associated diarrhoea. *Trends Microbiol* 2016;24:463–476.
9. Boyce JM, Havill NL. Nosocomial antibiotic-associated diarrhea associated with enterotoxin-producing strains of methicillin-resistant *Staphylococcus aureus*. *Am J Gastroenterol* 2005;100:1828–1834.
10. Fremont DH, Hendrickson WA, Marrack P, Kappler J. Structures of an MHC class II molecule with covalently bound single peptides. *Science* 1996;272:1001–1004.
11. Yeung RS, Penninger JM, Kündig T, Khoo W, Ohashi PS *et al*. Human CD4 and human major histocompatibility complex class II (DQ6) transgenic mice: supersensitivity to superantigen-induced septic shock. *Eur J Immunol* 1996;26:1074–1082.
12. Lu J, Wang A, Ansari S, Hershberg RM, McKay DM. Colonic bacterial superantigens evoke an inflammatory response and exaggerate disease in mice recovering from colitis. *Gastroenterology* 2003;125:1785–1795.
13. Pérez-Bosque A, Moretó M. A rat model of mild intestinal inflammation induced by *Staphylococcus aureus* enterotoxin B. *Proc Nutr Soc* 2010;69:447–453.
14. Misawa Y, Kelley KA, Wang X, Wang L, Park WB *et al*. *Staphylococcus aureus* colonization of the mouse gastrointestinal tract Is modulated by wall teichoic acid, capsule, and surface proteins. *PLoS Pathog* 2015;11:e1005061.
15. Gries DM, Pultz NJ, Donskey CJ. Growth in cecal mucus facilitates colonization of the mouse intestinal tract by methicillin-resistant *Staphylococcus aureus*. *J Infect Dis* 2005;192:1621–1627.
16. Holtfreter S, Radcliff FJ, Grumann D, Read H, Johnson S *et al*. Characterization of a mouse-adapted *Staphylococcus aureus* strain. *PLoS One* 2013;8:e71142.
17. Flaxman A, van Diemen PM, Yamaguchi Y, Allen E, Lindemann C *et al*. Development of persistent gastrointestinal *S. aureus* carriage in mice. *Sci Rep* 2017;7:12415.
18. Uramatsu M, Matsumoto T, Tateda K, Shibuya K, Miyazaki S *et al*. Involvement of endotoxin in the mortality of mice with gut-derived

sepsis due to methicillin-resistant *Staphylococcus aureus*. *Microbiol Immunol* 2010;54:330–337.

19. Lyon SA, Hutton ML, Rood JI, Cheung JK, Lyras D. CdtR regulates TcdA and TcdB production in *Clostridium difficile*. *PLoS Pathog* 2016;12:e1005758.
20. Larcombe S, Hutton ML, Riley TV, Abud HE, Lyras D. Diverse bacterial species contribute to antibiotic-associated diarrhoea and gastrointestinal damage. *J Infect* 2018;77:417–426.
21. Yao J, Zhong J, Fang Y, Geisinger E, Novick RP *et al*. Use of targetrons to disrupt essential and nonessential genes in *Staphylococcus aureus* reveals temperature sensitivity of LI.LtrB group II intron splicing. *RNA* 2006;12:1271–1281.
22. Pérez-Bosque A, Amat C, Polo J, Campbell JM, Crenshaw J *et al*. Spray-dried animal plasma prevents the effects of *Staphylococcus aureus* enterotoxin B on intestinal barrier function in weaned rats. *J Nutr* 2006;136:2838–2843.
23. Bateman BT, Donegan NP, Jarry TM, Palma M, Cheung AL. Evaluation of a tetracycline-inducible promoter in *Staphylococcus aureus in vitro* and *in vivo* and its application in demonstrating the role of *sigB* in microcolony formation. *Infect Immun* 2001;69:7851–7857.
24. Kreiswirth BN, Löfdahl S, Betley MJ, O'Reilly M, Schlievert PM *et al*. The toxic shock syndrome exotoxin structural gene is not detectably transmitted by a prophage. *Nature* 1983;305:709–712.
25. Monk IR, Shah IM, Xu M, Tan MW, Foster TJ. Transforming the untransformable: application of direct transformation to manipulate genetically *Staphylococcus aureus* and *Staphylococcus epidermidis*. *mBio* 2012;3:e00277–11.
26. Moolenbeek C, Ruitenberg EJ. The "Swiss roll": a simple technique for histological studies of the rodent intestine. *Lab Anim* 1981;15:57–60.
27. Larsen MV, Cosentino S, Rasmussen S, Friis C, Hasman H *et al*. Multilocus sequence typing of total-genome-sequenced bacteria. *J Clin Microbiol* 2012;50:1355–1361.
28. Bartels MD, Petersen A, Worning P, Nielsen JB, Larner-Svensson H *et al*. Comparing whole-genome sequencing with Sanger sequencing for *spa* typing of methicillin-resistant *Staphylococcus aureus*. *J Clin Microbiol* 2014;52:4305–4308.
29. Hutton ML, Cunningham BA, MacKin KE, Lyon SA, James ML *et al*. Bovine antibodies targeting primary and recurrent *Clostridium difficile* disease are a potent antibiotic alternative. *Sci Rep* 2017;7:3665.
30. Carter GP, Chakravorty A, Pham Nguyen TA, Mileto S, Schreiber F *et al*. Defining the roles of TcdA and TcdB in localized gastrointestinal disease, systemic organ damage, and the host response during *Clostridium difficile* infections. *mBio* 2015;6:e00551.
31. Squire MM, Carter GP, Mackin KE, Chakravorty A, Norén T *et al*. Novel molecular type of *Clostridium difficile* in neonatal pigs, Western Australia. *Emerg Infect Dis* 2013;19:790–792.
32. Li M, Diep BA, Villaruz AE, Braughton KR, Jiang X *et al*. Evolution of virulence in epidemic community-associated methicillin-resistant *Staphylococcus aureus*. *Proc Natl Acad Sci USA* 2009;106:5883–5888.
33. Sieradzki K, Leski T, Dick J, Borio L, Tomasz A. Evolution of a vancomycin-intermediate *Staphylococcus aureus* strain *in vivo*: multiple changes in the antibiotic resistance phenotypes of a single lineage of methicillin-resistant *S. aureus* under the impact of antibiotics administered for chemotherapy. *J Clin Microbiol* 2003;41:1687–1693.
34. Endt K, Stecher B, Chaffron S, Slack E, Tchitchek N *et al*. The microbiota mediates pathogen clearance from the gut lumen after non-typhoidal *Salmonella* diarrhea. *PLoS Pathog* 2010;6:e1001097.
35. Kamada N, Seo SU, Chen GY, Núñez G. Role of the gut microbiota in immunity and inflammatory disease. *Nat Rev Immunol* 2013;13:321–335.
36. Kernbauer E, Maurer K, Torres VJ, Shopsin B, Cadwell K. Gastrointestinal dissemination and transmission of *Staphylococcus aureus* following bacteremia. *Infect Immun* 2015;83:372–378.
37. Ashida H, Ogawa M, Kim M, Mimuro H, Sasakawa C. Bacteria and host interactions in the gut epithelial barrier. *Nat Chem Biol* 2011;8:36–45.
38. Pinchuk IV, Beswick EJ, Reyes VE. Staphylococcal enterotoxins. *Toxins* 2010;2:2177–2197.
39. Shupp JW, Jett M, Pontzer CH. Identification of a transcytosis epitope on staphylococcal enterotoxins. *Infect Immun* 2002;70:2178–2186.
40. Casaletto JB, Saotome I, Curto M, McClatchey AI. Ezrin-mediated apical integrity is required for intestinal homeostasis. *Proc Natl Acad Sci USA* 2011;108:11924–11929.
41. Hutton ML, MacKin KE, Chakravorty A, Lyras D. Small animal models for the study of *Clostridium difficile* disease pathogenesis. *FEMS Microbiol Lett* 2014;352:140–149.